Low-energy $\bar{K}N$ interactions

B. Borasoy [a,b], R. Nißler [a,b] and W. Weise [a]

[a]Physik Department, Technische Universität München

D-85747 Garching, Germany

[b]Helmholtz-Institut für Strahlen- und Kernphysik,

Universität Bonn, D-53115 Bonn, Germany

Chiral SU(3) effective field theory in combination with a relativistic coupled-channels approach is used to perform a novel analysis of the strong interaction shift and width in kaonic hydrogen in view of the new accurate DEAR measurements. Questions of consistency with previous K^-p data are examined. Coulomb and isospin breaking effects are shown to be important.

1 Motivation

The low-energy $\bar{K}N$ system is of special interest as a testing ground for chiral SU(3) symmetry in QCD and, in particular, for the role of explicit symmetry breaking induced by the relatively large mass of the strange quark. Most significantly, the existence of the $\Lambda(1405)$ resonance just 25 MeV below the K^-p threshold makes the loopwise expansion of chiral perturbation theory inapplicable in this channel. Non-perturbative coupled-channel techniques based on driving terms of the chiral SU(3) effective Lagrangian have proved useful and successful in dealing with this problem, by generating the $\Lambda(1405)$ dynamically as an $I = 0$ $\bar{K}N$ quasibound state and as a resonance in the $\pi\Sigma$ channel. High-precision K^-p threshold data set important constraints for such theoretical approaches. Now that new accurate results for the strong interaction shift and width of kaonic hydrogen from the DEAR experiment [1] are available, there is renewed interest in an improved analysis of these data along with existing information on K^-p scattering, the $\pi\Sigma$ mass spectrum and K^-p threshold decay ratios. The results of this work are presented in detail in [2].

2 Formalism

Chiral perturbation theory (ChPT) is an appropriate framework to investigate the dynamics of hadrons at low energies, whereby symmetries and symmetry breaking patterns

of QCD are incorporated. A systematic loop expansion can be carried out, but its perturbative application is often limited to a small range of energies and breaks down in the vicinity of resonances such as, e.g, the $\Lambda(1405)$ resonance just below the K^-p threshold.

In such cases, the combination with non-perturbative coupled-channels techniques provides a suitable theoretical framework which has been applied to a variety of meson-baryon scattering processes with quite some success [3, 4, 5, 6, 7, 8, 9, 10]. All those calculations appear to describe the available scattering data similarly well, whereas the details of the chosen framework, e.g. the driving terms in the Bethe-Salpeter equation, usually differ. To our knowledge no attempt has so far been made to compare the different approaches systematically. To this end, we study in the present work several variants of the coupled-channels approaches to the $\bar{K}N$ system with different interaction kernels, hence providing an estimate for the model dependence of such analyses.

The starting point is the chiral effective Lagrangian $\mathcal{L} = \mathcal{L}_\phi + \mathcal{L}_{\phi B}$ which describes the coupling of the pseudoscalar meson octet (π, K, η) to the ground state baryon octet $(N, \Lambda, \Sigma, \Xi)$. The mesonic piece $\mathcal{L}_\phi$ is employed up to second chiral order [11], whereas the second part $\mathcal{L}_{\phi B}$ of the Lagrangian describes the meson-baryon interactions at next-to-leading order [12].

For $\bar{K}N$ scattering unitarity effects from final state interactions are important due to the nearby $\Lambda(1405)$ resonance and must be included in a non-perturbative fashion. To this end, one computes from the Lagrangian the relativistic tree level amplitude $V_{jb,ia}(s, \Omega; \sigma, \sigma')$ of the meson-baryon scattering processes $\phi_i B_a^\sigma \to \phi_j B_b^{\sigma'}$ (with spin indices σ, σ'). This amplitude is the driving term in the coupled-channels integral equation determining the meson-baryon T-matrix.

The effective meson-baryon Lagrangian has been used at different levels of sophistication in the literature. While only the Weinberg-Tomozawa term from the covariant derivative is taken, e.g., in [4], the direct and crossed Born terms are included in [6]. In [5] the Lagrangian of second chiral order is added which yields additional contact interactions, whereas in [8] the contact interactions and the direct Born term have been taken into account, but the crossed Born term has been excluded. In order to provide an estimate of the model-dependence of such approaches, we will discuss the following four different choices for the amplitude $V_{jb,ia}(s, \Omega; \sigma, \sigma')$.

First, only the leading order contact (Weinberg-Tomozawa) term is taken into account, see Figure 1a. Subsequently, the contact interactions from the Lagrangian of second chiral order, $\mathcal{L}_{\phi B}^{(2)}$, are included, see Fig. 1b. In the third and fourth approach we add successively the direct (Fig. 1c) and crossed (Fig. 1d) Born diagrams. For brevity, we will refer to these variants as "WT" (Weinberg-Tomozawa), "c" (additional contact terms), "s" (including s-channel Born diagram) and "u" (including u-channel Born diagram), respectively.

It turns out that already the inclusion of the next-to-leading order contact terms, which have been neglected in many previous coupled-channel analyses [4, 6, 7, 9], improves the agreement of our results with the well-measured K^-p threshold branching ratios and the shape of the $\pi\Sigma$ mass spectrum, whereas the Born diagrams Fig. 1c,d yield only small numerical changes.

Since we are primarily concerned with a narrow center-of-mass energy region around the $\bar{K}N$ threshold, it is sufficient to restrict ourselves to the s-wave (matrix) amplitude $V(s)$. For each partial wave l unitarity imposes a restriction on the (inverse) T-matrix

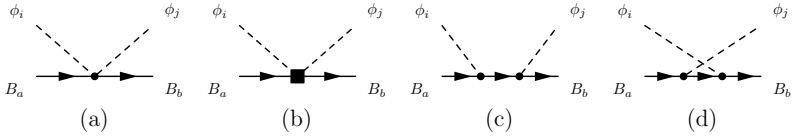

Figure 1: Shown are the leading order (a) and next-to-leading order (b) contact interactions as well as the direct (c) and crossed (d) Born terms. Solid and dashed lines represent baryons and pseudoscalar mesons, respectively.

above the pertinent thresholds

$$\mathrm{Im}T_l^{-1} = -\frac{|\mathbf{q}_{cm}|}{8\pi\sqrt{s}} \tag{1}$$

with $\mathbf{q}_{cm}$ being the three-momentum in the center-of-mass frame of the channel under consideration. To the order we are working the inverse of the T matrix can be written as (suppressing the subscript l $(= 0)$ for brevity)

$$T^{-1} = V^{-1} + G \ , \tag{2}$$

which yields after inversion

$$T = [1 + V \cdot G]^{-1} \, V. \tag{3}$$

The quantity G is the finite part of the scalar loop integral $\tilde{G}$

$$\tilde{G}(q^2) = \int \frac{d^dp}{(2\pi)^d} \frac{i}{[(q-p)^2 - M_B^2 + i\epsilon][p^2 - m_\phi^2 + i\epsilon]} \ , \tag{4}$$

where M_B and m_ϕ are the physical masses of the baryon and the meson, respectively. Eq. (3) is a matrix equation with the diagonal matrix G collecting the loop integrals in each channel. This amounts to a summation of a bubble chain to all orders in the s-channel, equivalent to solving a Bethe-Salpeter equation with V as driving term, where all momenta in V are set to their on-shell values. This so-called on-shell scheme reduces the full Bethe-Salpeter equation to the simple matrix equation (3).

Moreover, the Coulomb interaction has been shown to yield significant contributions to the elastic K^-p scattering amplitude up to kaon laboratory momenta of 100-150 MeV/c [13]. Close to K^-p threshold the electromagnetic interactions are thus important as well and should not be neglected as in previous coupled-channel calculations [4, 5, 6, 7, 9]. We account for the electromagnetic interaction by adding the quantum mechanical Coulomb scattering amplitude to the strong elastic K^-p amplitude.

3 Results and discussion

In this section we present and discuss the numerical results of our calculation. Low-energy antikaon-nucleon scattering and reactions have been studied experimentally decades ago [14, 15, 16, 17, 18, 19]. The available data (admittedly with large errors) are mostly restricted to K^- momenta above 100 MeV/c. On the other hand, there is the new and

precise DEAR measurement of the strong interaction shift and width in kaonic hydrogen [1] as well as a similar recent analysis of the KEK collaboration [25], which set constraints for the strong-interaction part of the elastic K^-p amplitude at threshold. Further tight constraints are imposed by the accurately determined threshold branching ratios into the inelastic channels $\pi\Sigma$ and $\pi^0\Lambda$ [20, 21] and by the $\pi\Sigma$ invariant mass spectrum in the isospin $I = 0$ channel [22].

In the first part of this section, we compare the four different approaches described in the preceding section which follow from the successive inclusion of the diagrams in Fig. 1 in the interaction kernel V. It turns out that in all four cases the results cannot be brought into simultaneous satisfactory agreement with the elastic K^-p elastic cross section and the kaonic hydrogen data from the DEAR experiment [1], although the inclusion of the Coulomb interaction ameliorates the situation compared to previous coupled-channel calculations. In order to examine how well the four approaches under consideration agree with the scattering data, we first exclude the DEAR data from the fit and "predict" the strong-interaction shift and width in kaonic hydrogen based on the rest of the low-energy scattering data.

As a second step, we then investigate the changes of the results when the DEAR data are included in the fit. For this purpose it is sufficient to restrict ourselves to the "u" ansatz involving all the diagrams in Fig. 1—i.e. the entire set of next-to-leading order contributions to the s-wave amplitude—since qualitatively similar results are obtained in the "c" and "s" models.

3.1 Comparison of the different approaches

We have first performed an overall χ^2 fit to the available low energy $\bar{K}N$ data excluding the strong level shift and width of kaonic hydrogen. In Fig. 2 we show the results for the elastic and inelastic cross sections of K^-p scattering. The four lines correspond to the four different approaches under consideration, all of them in good agreement with the experimental data. The $\pi\Sigma$ mass spectrum and the K^-p threshold branching ratios are also well reproduced, although the agreement is slightly less satisfactory in the "WT" approach.

Having so far omitted the strong interaction shift and width in kaonic hydrogen from the fits, we can now predict these observables for the different approaches. To this end we employ the result of [23] relating the ground state strong energy shift ΔE and width Γ of kaonic hydrogen to the K^-p scattering length a_{K^-p} in the presence of electromagnetic corrections:

$$\Delta E - \frac{i}{2}\Gamma = -2\alpha^3\mu_c^2 a_{K^-p}\left[1 - 2\alpha\mu_c(\ln\alpha - 1)a_{K^-p}\right] . \tag{5}$$

The reduced mass of the K^-p system is denoted by μ_c, α is the fine-structure constant, and the scattering length a_{K^-p} is given by the strong interaction T matrix at threshold

$$a_{K^-p} = \frac{1}{8\pi\sqrt{s}}\, T_{K^-p\to K^-p}(s)|_{s=(m_{K^-}+M_p)^2} . \tag{6}$$

In order to demonstrate the importance of the electromagnetic corrections calculated in [23], we compare Eq. (5) with the predictions derived from the well-known Deser-Trueman

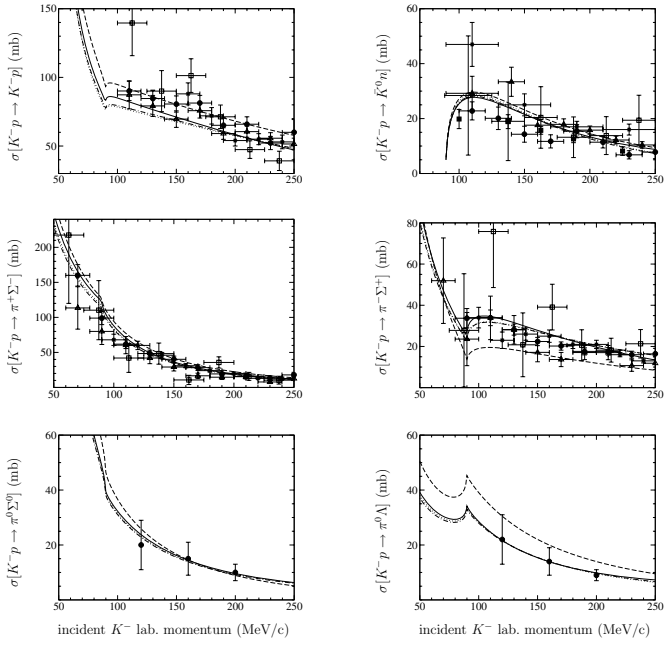

Figure 2: Total cross sections for K^-p scattering into various channels. The data are taken from [14] (empty squares), [15] (empty triangles), [16] (filled circles), [17] (filled squares), [18] (filled triangles), [19] (stars). The dashed, dotted, dot-dashed and solid lines correspond to the approaches "WT", "c", "s" and "u", respectively.

formula [24]

$$\Delta E - \frac{i}{2}\Gamma = -2\alpha^3\mu_c^2 a_{K^-p} \tag{7}$$

and the kaonic hydrogen data from the DEAR [1] and KEK [25] experiments in Fig. 3. The shifts and widths corresponding to the different approaches agree all with the error ranges given in [25] if Eq. (5) is utilized. In contrast, both the shift and the width of the new DEAR experiment cannot be accommodated by the coupled-channels approaches constrained by scattering and reaction cross sections, although the electromagnetic corrections given in [23] reduce the width Γ by a significant amount. As can be seen in Fig. 3 the disagreement is reduced by the inclusion of higher order contact terms (approaches "c", "s", "u").

In summary we note that the approaches which include the next-to-leading order contact terms ("c", "s", "u") describe all available low energy hadronic scattering data excluding kaonic hydrogen experiments at DEAR. The fits to the $K^-p \to \pi^-\Sigma^+$ cross section and the related branching ratio which we obtain within the "WT" approach are not of the same high quality. One should keep in mind however that the leading order "WT" framework is oversimplified and does not involve the next-to-leading order coupling

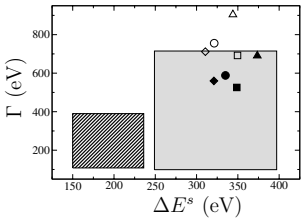

Figure 3: Predictions for the strong interaction shift and width of kaonic hydrogen from the different approaches both by using the Deser-Trueman formula, Eq. (7), (empty symbols) and by including isospin breaking corrections, Eq. (5), (filled symbols). The "WT", "c", "s" and "u" approach is depicted by triangles, diamonds, squares and circles, respectively. The DEAR data are represented by the shaded box [1], the KEK data by the light gray box [25].

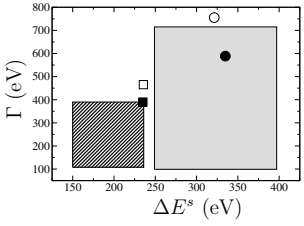

Figure 4: Results for the strong interaction shift and width of kaonic hydrogen from the fits "1" and "2" depicted by circles and squares. Empty symbols correspond to the Deser-Trueman formula, Eq. (7), full symbols to Eq. (5), where isospin breaking corrections are included. The DEAR data are represented by the shaded box [1], the KEK data by the light gray box [25].

constants which turn out to be important in the more complete approaches.

3.2 Inclusion of the DEAR data

Apparently, the new high-precision DEAR data [1] set additional tight constraints on $\bar{K}N$ interactions. In this section we explore changes of our results when the DEAR data are included in the fit. For brevity we restrict ourselves to the discussion of the "u" scheme. We utilize this "u" fit and rename it "1". Forcing the fit to strictly remain within the error range given by the DEAR experiment we obtain result "2", see Fig. 4.

Total cross sections of K^-p scattering into various channels are shown in Fig. 5. Deviations between fit "2" (which satisfies the DEAR constraints) and fit "1" (where these constraints have been omitted) are most pronounced in the elastic channel $K^-p \to K^-p$. While there might be questions about the detailed treatment of Coulomb corrections, these effects can safely be neglected for kaon momenta above 200 MeV/c. Our findings suggest that within coupled-channels schemes constrained by large amounts of data, the new accurate DEAR results and the old elastic K^-p scattering cross sections at low energy

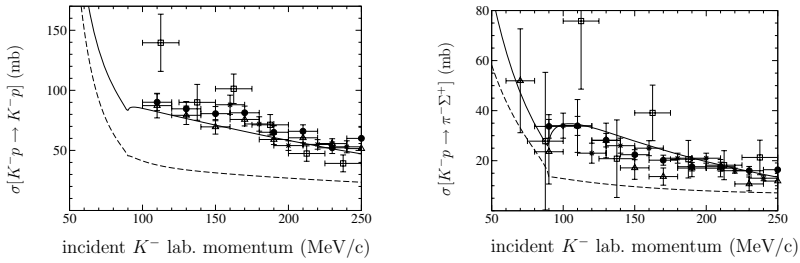

Figure 5: Total cross sections of K^-p scattering into K^-p and $\pi^-\Sigma^+$. The data are taken from [14] (empty squares), [15] (empty triangles), [16] (filled circles), [19] (stars). The solid and dashed lines represent the fits "1" and "2", respectively.

cannot be simultaneously accommodated.

As pointed out in [26] $\Lambda(1405)$ photoproduction, which has been investigated experimentally at SPring-8 [27] and at ELSA, could serve as a tool to constrain $\bar{K}N$ dynamics below threshold. If t-channel exchange of K^- mesons can be isolated, it should be possible to extract from the process $\gamma p \to K^+\pi\Sigma$ the $K^-p \to \pi\Sigma$ amplitudes below the K^-p threshold. This statement is also of interest for the present investigation, since the fits which either in- or exclude the DEAR data yield different predictions for these amplitudes. In Fig. 6 we plot the quantity $4\,|\mathbf{q}_{cm}^{K^-p}|\sqrt{s}\;\sigma_{K^-p\to\pi^\mp\Sigma^\pm}(s)$ continued below threshold, and the experimental cross section data above the K^-p threshold have been normalized accordingly. In the case of fit "2", the one consistent with the DEAR data, the shape of the curve is altered for both final states $\pi^-\Sigma^+$ and $\pi^+\Sigma^-$. Compared to fit "1" the peak position is shifted to lower energies, while the width is considerably increased. This difference can be examined experimentally once the necessary t-channel analysis and normalization of the SPring-8 results [27] has been performed. These data cover an energy range from the $\pi\Sigma$ threshold up to energies above the K^-p threshold, where consistency with existing cross section data can be tested. In conclusion, the SPring-8/ELSA experiments may provide a further important consistency check of scattering data and the DEAR results within our framework.

4 Conclusions

In the present work, we have critically examined and updated the analysis of the $\bar{K}N$ system within the framework of coupled-channels approaches combined with chiral SU(3) dynamics. There is renewed interest in the investigation of the $\bar{K}N$ channel in the light of the new accurate measurement of the strong interaction shift and width of kaonic hydrogen at DEAR which sets tight constraints. It is therefore worth investigating whether both the DEAR data and the K^-p scattering data can be accommodated by coupled-channels analyses, while at the same time trying to reduce the inherent model dependence of these approaches wherein chiral effective field theory is combined with a non-perturbative Bethe-Salpeter equation. The driving terms for the Bethe-Salpeter equation are derived from the effective Lagrangian and constitute a major source of model dependence. Several

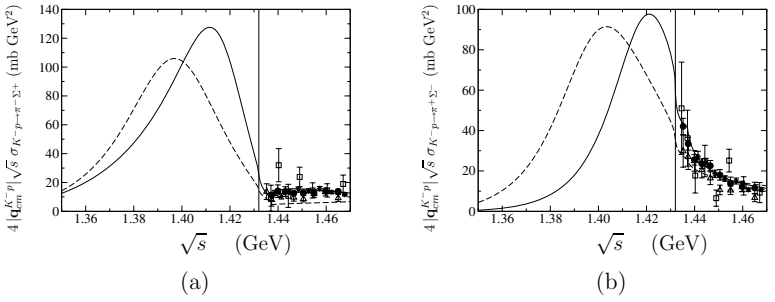

Figure 6: Shown are the cross sections for $K^-p \to \pi^-\Sigma^+$ (a) and $K^-p \to \pi^+\Sigma^-$ (b) multiplied by $4|\mathbf{q}_{cm}^{K^-p}|\sqrt{s}$ and continued below K^-p threshold (vertical line). The experimental data points are the same as in Fig. 2, but have been modified accordingly. The solid and dashed lines correspond to the fits "1" and "2", respectively.

variants of such approaches are commonly used in the literature, e.g., only the Weinberg-Tomozawa term originating from the leading order Lagrangian is taken into account, while in other works direct and crossed Born terms are added or contact interactions of the next-to-leading chiral order are included.

In the present investigation, we have worked out the driving terms in four consecutive steps. Starting from the Weinberg-Tomozawa term, we successively added contact interactions of second chiral order, the direct Born term and the crossed Born term. All four versions have in common that the agreement with $\bar{K}N$ scattering data is partly spoilt once the new tight constraints imposed by the DEAR experiment are taken into account. (We mention though that the results of these models fall within the larger error ranges of the KEK experiment.) The largest discrepancies are observed in the elastic K^-p channel where the calculated cross section is substantially lowered by inclusion of the DEAR data. Coulomb effects ameliorate the situation at low kaon laboratory momenta below 100 MeV/c, but an offset to elastic K^-p scattering data remains. Moreover, electromagnetic corrections to the strong interaction shift and width in kaonic hydrogen as given in [23] reduce the discrepancy further, but are not able to compensate the difference between the coupled-channels approaches and the experimental data. Further tight phenomenological constraints in the $\bar{K}N$ system are provided by the threshold branching ratios which have been measured very precisely. Inclusion of the DEAR data produces results for the branching ratios which are not in agreement with the quoted experimental error ranges.

Another consistency check could be provided by studying the $K^-p \to \pi\Sigma$ amplitude below the K^-p threshold, since inclusion of the DEAR data amounts to a substantial change in this amplitude. Experiments towards this direction are currently analyzed at SPring-8/LEPS and at ELSA, where photoproduction of $\Lambda(1405)$ has been measured. If K^- exchange in the t-channel can be isolated from these data, the information gained would be very useful in order to set constraints for the $\bar{K}N$ scattering amplitude below threshold [26].

The comparison between the different variants of the coupled-channels approaches can

be summarized as follows. The quality of the fits to data is improved substantially by including next-to-leading order contact interactions with new parameters of the effective Lagrangian. The inclusion of the Born terms, on the other hand, leads only to minor changes. The treatment of the interaction kernel at subleading order also destroys the pronounced double pole structure of the $\Lambda(1405)$ close to the real axis as observed in [9]. Although we still see two poles in the relevant unphysical sheet, the pole with a stronger coupling to the $\pi\Sigma$ channel now moves far away from the real axis, losing its importance for any physical observables. As a consequence, the full partial wave amplitude for $\pi\Sigma \to \pi\Sigma$ is not approximated well by just these two poles and the background contribution becomes important.

The updated, constrained analysis presented here is also of considerable interest in the discussion of possible deeply bound K^-- nuclear states [28]. The amplitudes obtained for elastic $K^-p \to K^-p$ scattering suggest a complex, energy dependent subthreshold $\bar{K}$-nucleus potential which is attractive in the $\bar{K}N$ energy range below the $\Lambda(1405)$. Its imaginary part decreases as the energy is lowered towards the $\pi\Sigma$ threshold, an effect that has been pointed out previously in Refs. [29]. This is a potential mechanism for supporting narrow bound $\bar{K}$ states at sufficiently large nuclear densities, but details concerning the strong energy dependence of the driving potentials require additional constraints and further investigation.

Acknowledgments

It is a pleasure to thank the organizers for this pleasant and stimulating conference. Partial financial support by DFG and BMBF is gratefully acknowledged. This research is part of the EU Integrated Infrastructure Initiative Hadronphysics under contract number RII3-CT-2004-506078.

References

[1] M. Cargnelli et al. (DEAR collaboration), Int. J. Mod. Phys. **A20** (2005) 341.
[2] B. Borasoy, R. Nißler, and W. Weise, Phys. Rev. Lett. (in print), hep-ph/0410305; B. Borasoy, R. Nißler, and W. Weise, preprint TUM/T39-05-04 and HISKP-TH-05/12.
[3] N. Kaiser, P. B. Siegel, and W. Weise, Nucl. Phys. **A594** (1995) 325.
[4] E. Oset, A. Ramos, Nucl. Phys. **A635** (1998) 99.
[5] N. Kaiser, P. B. Siegel, and W. Weise, Phys. Lett. **B362** (1995) 23; N. Kaiser, T. Waas, and W. Weise, Nucl. Phys. **A612** (1997) 297; J. Caro Ramon, N. Kaiser, S. Wetzel, and W. Weise, Nucl. Phys. **A672** (2000) 249.
[6] J. A. Oller and U.-G. Meißner, Phys. Lett. **B500** (2001) 263.
[7] M. F. M. Lutz and E. Kolomeitsev, Nucl. Phys. **A700** (2002) 193.
[8] B. Borasoy, E. Marco, and S. Wetzel, Phys. Rev. **C66** (2002) 055208.
[9] D. Jido, J. A. Oller, E. Oset, A. Ramos, and U. G. Meißner, Nucl. Phys. **A725** (2003) 181.

[10] A. Bahaoui, C. Fayard, T. Mizutani, and B. Saghai, Phys. Rev. **C68** (2003) 064001.
[11] J. Gasser and H. Leutwyler, Nucl. Phys. **B250** (1985) 465.
[12] A. Krause, Helv. Phys. Acta **63** (1990) 3.
[13] J. C. Jackson and H. W. Wyld, Phys. Rev. Lett. **8** (1959) 355;
R. H. Dalitz and S. F. Tuan, Ann. Phys. **10** (1960) 307.
[14] W. E. Humphrey and R. R. Ross, Phys. Rev. **127** (1962) 1305.
[15] M. Sakitt *et al.*, Phys. Rev. **139** (1965) B719.
[16] J. K. Kim, Phys. Rev. Lett. **14** (1965) 29; Columbia University Report, Nevis **149** (1966); Phys. Rev. Lett. **19** (1967) 1074.
[17] W. Kittel, G. Otter, and I. Wacek, Phys. Lett. **21** (1966) 349.
[18] D. Evans *et al.*, J. Phys. **G9** (1983) 885.
[19] J. Ciborowski *et al.*, J. Phys. **G8** (1982) 13.
[20] R. J. Nowak *et al.*, Nucl. Phys. **B139** (1978) 61.
[21] D. N. Tovee *et al.*, Nucl. Phys. **B33** (1971) 493.
[22] R. J. Hemingway, Nucl. Phys. **B253** (1985) 742.
[23] U.-G. Meißner, U. Raha, and A. Rusetsky, Eur. Phys. J. **C35** (2004) 349.
[24] S. Deser, M. L. Goldberger, K. Baumann, and W. Thirring, Phys. Rev. **96** (1954) 774;
T. L. Trueman, Nucl. Phys. **26** (1961) 57.
[25] M. Iwasaki *et al.*, Phys. Rev. Lett. **78** (1997) 3067;
T. M. Ito *et al.*, Phys. Rev. **C58** (1998) 2366.
[26] M. F. M. Lutz and M. Soyeur, Nucl. Phys. **A748** (2005) 499.
[27] J. K. Ahn, Nucl. Phys. **A721** (2003) 715c.
[28] A. Dote, Y. Akaishi, and T. Yamazaki, Prog. Theor. Phys. Suppl. **156** (2004) 184.
[29] T. Waas, N. Kaiser, and W. Weise, Phys. Lett. **B379** (1996) 34;
T. Waas, M. Rho, and W. Weise, Nucl. Phys. **A617** (1997) 449;
T. Waas and W. Weise, Nucl. Phys. **A625** (1997) 287.